Role of interactions in an electronic Fabry–Perot interferometer operating in the quantum Hall effect regime

Nissim Ofek[1], Aveek Bid, Moty Heiblum, Ady Stern, Vladimir Umansky, and Diana Mahalu

Braun Center for Submicron Research, Department of Condensed Matter Physics, Weizmann Institute of Science, Rehovot 76100, Israel

Edited by Klaus von Klitzing, Max Planck Institute for Solid State Research, Stuttgart, Germany, and approved February 5, 2010 (received for review November 5, 2009)

Interference of edge channels is expected to be a prominent tool for studying statistics of charged quasiparticles in the quantum Hall effect (QHE). We present here a detailed study of an electronic Fabry–Perot interferometer (FPI) operating in the QHE regime [C. Chamon, et al. (1997) *Phys Rev B* 55:2331–2334], with the phase of the interfering quasiparticles controlled by the Aharonov–Bohm effect. Our main finding is that Coulomb interactions among the electrons dominate the interference, even in a relatively large area FPI, leading to a strong dependence of the area enclosed by the interference loop on the magnetic field. In particular, for a composite edge structure, with a few independent edge channels propagating along the edge, interference of the outmost edge channel (belonging to the lowest Landau level) was *insensitive* to magnetic field—suggesting a constant enclosed flux. However, when any of the inner edge channels interfered, the enclosed flux *decreased* when the magnetic field *increased*. By intentionally varying the enclosed area with a biased metallic gate and observing the periodicity of the interference pattern, charges *e* (for integer filling factors) and *e*/3 (for a fractional filling factor) were found to be expelled from the FPI. Moreover, these observations provided also a novel way of detecting the charge of the interfering quasiparticles.

Aharonov–Bohm | edge channels | fractional charge | interference

A considerable amount of work has been focused in recent years on interference of quantum particles, aiming at understanding "single-particle" as well as "correlated-particles" physics. Experiments were designed to measure the quantum coherence time (1), to determine phase of the scattering amplitudes (2), to test entanglement between a pair of quantum particles (3), and, more recently, to probe their charge and coherence properties in the integer and fractional quantum Hall effect (QHE) regimes (IQHE and FQHE, respectively) (4–8). However, even though the statistics of identical quantum particles upon exchange is at the core of many physical phenomena, experiments to directly observe this intrinsic property are scarce (4, 5). Recent interest in topological quantum computation (9–11) led to a series of theoretical proposals aimed at demonstrating the statistics of quasiparticles in the FQHE (12). The ideas are primarily based on performing interference in an electronic version of a Fabry–Perot interferometer (FPI) (13, 14) or in a similar Mach–Zehnder interferometer (MZI) (15, 16), with distinct "fingerprints" of the interfering quasiparticles. The MZI, although more difficult to fabricate, is a "true two-path" interferometer. On the other hand, in the FPI, which is a simpler device, many trajectories contribute to the interference. Understanding the physics governing these interferometers is crucial if they are to be used to probe the statistics of quasiparticles.

We performed a detailed study of an electronic FPI operating in the IQHE and the FQHE regimes. Different from previous works, our devices allowed the study of interference of any of the propagating edge channels, at integer and fractional filling factors, for a few areal carrier densities, the dependence on magnetic field, as function of the FPI area, and at different coupling strengths to the reservoir leads. Previous works (5, 17, 18) reported on more restricted phenomena (mostly on interference of the innermost channel), hence missing some of the more striking effects we report here. Moreover, our measurements in the FQHE regime are strikingly different from those of Goldman and coworkers (5), which have been difficult to interpret all along. Our data aims at attaining a rather complete picture of the behavior of the FPI in the QHE regime, with a particular focus on the role of electron–electron interaction that seem to dominate the interference.

Experimental Procedures

The electronic FPI, discussed in some detail first by Chamon et al. (14), was realized in a form of a Hall bar perturbed along the current flow by two constrictions, each formed by a biased split-gate quantum point contact (QPC), with a plunger gate that controlled the area of the FPI (shown in Fig. 1). Current flows chirally in the form of distinct edge channels, with the lower right-moving channel biased (at voltage V_{DS}) relative to the upper left-moving one (kept at ground potential). When the bulk is in a QHE state, the two-terminal conductance, in the absence of the constrictions, is quantized at $\nu \cdot e^2/h$, with $\nu = n\phi_0/B$ being the filling factor, where n is the areal electron density, $\phi_0 = h/e$ the flux quantum, e the electron charge, h the Planck constant, and B the magnetic field. Each constriction induces backscattering from a forward propagating edge channel to a backward moving one. Circulating edge currents in the FPI acquire a phase determined by the Aharonov–Bohm (AB) effect (proportional to the enclosed magnetic flux) and the number of enclosed quasiparticles. The AB phase can be controlled by either changing the magnetic field or the area of the interferometer (via biasing the plunger gate).

Our interferometers were fabricated on heterostructures embedding 2DEG with a few different areal electron densities, $n = 5.6 \times 10^{10}$, 8.6×10^{10}, and 2.0×10^{11} cm^{-2}, all having low-temperature mobility in excess of 10×10^6 cm^2/V-s. Measurements were done on two FPIs of different sizes, one with an area $\sim$4.4 μm^2 and one with an area $\sim$17.6 μm^2, with a plunger gate width of 0.4 μm. Here we present data mainly taken with the smaller FPI (unless otherwise specified), fabricated on the wafer with electron density 8.6×10^{10} cm^{-2} (the depth of the electron gas from the surface was 130 nm) (see Fig. 1*B*). Samples were cooled in a dilution refrigerator to an electron temperature $\sim$10 mK (verified by temperature sensitive shot noise measurements) with conductance measurements taken at a typical excitation voltage of about 1 μVp-p at 800 kHz. The parameters

N.O., A.B., and M.H. designed research; N.O., A.B. V.U., and D.M. performed research; N.O. and A.B. analyzed data; and N.O., A.B., M.H., and A.S. wrote the paper.

The authors declare no conflict of interest.

This article is a PNAS Direct Submission.

[1]To whom correspondence should be addressed. E-mail: nissim.ofek@weizmann.ac.il.

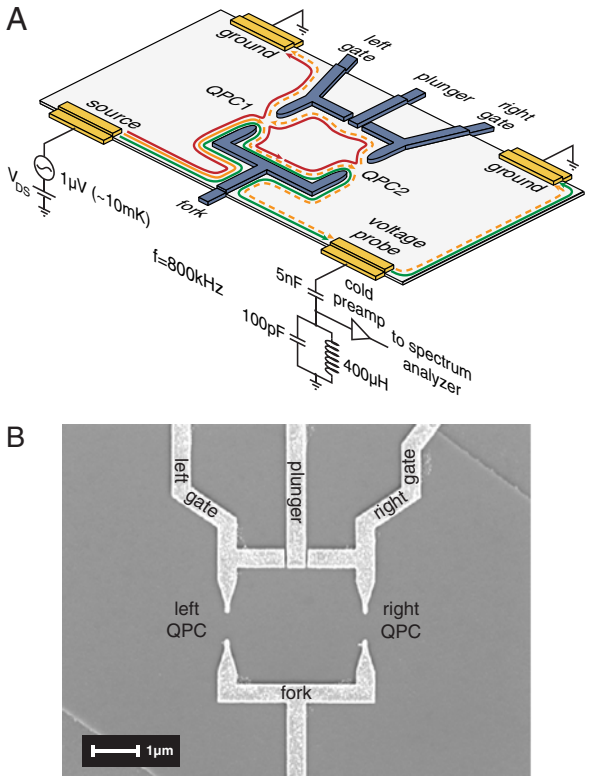

Fig. 1. Measurement circuit and the Fabry–Perot interferometer. (*A*) A cell of 2DEG confined by two quantum point contacts constrictions, with transmissions t_i (reflection $r_i = 1 - t_i$) determining the confinement of the electrons. Measurements are carried out with the bulk in a quantum Hall plateau, with a constant voltage source ~1 μVp-p at 800 kHz. The voltage measured at the voltage probe is proportional to the transmission probability through the interferometer. An optional top gate covers a portion of the cell (see Figs. 4 and 8). (*B*) SEM image of the FPI where the bright regions are the metallic gates. The cell area, after taking into account a depletion width of 250 nm, is about 4.4 μm^2.

of the system are as follows: the area of the interferometer, A; the magnetic field, B; the QPCs split-gate voltages, V_{QPC1} and V_{QPC2}; the plunger gate voltage, V_g; the bias on the source, V_{DS}; the electron temperature, T; and, in some devices, the voltage applied to a top gate, V_{TG}.

The cell of the FPI is defined by depleting the electrons underneath the metallic gates that surrounds it while assuring that the two constrictions stay open. Then, the magnetic field is tuned to the approximate center of a conductance plateau, with the filling factor in the FPI cell similar to that in the bulk (verified by multiterminal Hall measurements across the interferometer). The constrictions are then being carefully pinched (via the split-gate voltages, V_{QPC1} and V_{QPC2}), resulting in transmissions of the interfering edge channel t_1 and t_2, respectively. We denote the number of fully reflected edge channels, belonging to the highest Landau levels, being also the number of circulating edge channels within the FPI cell, by f_R, and the number of fully transmitted edge channels, belonging to the lowest Landau levels, by f_T. Together with the interfering channel, the total number of channels is $f_{edge} = f_T + 1 + f_R$, being determined by the bulk filling factor ν (for IQHE, $f_{edge} = \nu$). We notate each configuration as $(\nu, f_T) \equiv$(bulk filling factor, number of fully transmitted edge channels). The two-terminal differential conductance $\partial I/\partial V_{DS}$ was measured as function of various parameters, $\partial I/\partial V_{DS}$ (B, V_g, f_T, t_1, t_2), from which the periodicities of the AB oscillations were extracted, ΔB (B, V_g, f_T, t_1, t_2) $(\Delta B \ll B)$ and ΔV_g (B, V_g, f_T, t_1, t_2). We have selected only a subset of our results to present here, which, however, portray a rather complete picture of the behavior of the FPI.

Results

In the IQHE regime, interference was measured for all possible configurations (ν, f_T), with $f_T = 1 \ldots \nu - 1$ and $\nu = 1$–6 and at different settings of transmissions t_1 and t_2. As expected, for t_1, $t_2 \ll 1$ (weak coupling to the leads), multiple reflected trajectories within the FPI interfered, and the two-terminal conductance peaked sharply as function of flux; wheras at high transmissions t_1 and t_2, the conductance was almost sinusoidal as function of flux. However, and this is important to note, the periodicities of the interference were independent of the transmissions.

We start with (1, 0), namely, a single propagating edge channel (the spin resolved first Landau level), with an oscillating conductance as function of V_g, with periodicity $\Delta V_g = 2.35$ mV (Fig. 2 *Inset*).

Remarkably, the conductance in this case (and universally for all cases of $f_T = 0$) was found to be independent of magnetic field for many added flux quanta (the magnetic field corresponding to one flux quantum threading 4.4 μm^2 is ~9.8 G). So here we had an extraordinary situation where AB oscillations were responsive to a change in area but not to a change in the threading magnetic field. In contrast, profound oscillations as function of both B and V_g were always observed for $f_T > 0$, with a typical behavior for case (3, 2) shown in Fig. 3. The periodicity with V_g was found to depend only on f_T (in both the IQHE and FQHE regimes), increasing when f_T increased. The slope of the constant phase lines in the B-V_g plane is intriguing: *an increase* in B *must be accompanied by an increase* in V_g in order to keep the phase constant (as was also observed in ref. 18). This suggests that an increase in B leads to a decrease of the enclosed flux—an opposite behavior to that observed before in the electronic MZI (15). An exception to this behavior, observed in our large FPI, will be discussed separately. In the example in Fig. 3*A* [case (3, 2)], the dependence of the transmission on B and on V_g was sinusoidal for large t_1 and t_2, becoming an array of periodic sharp peaks when the constrictions were pinched (Fig. 3*B*), however, the periodicities did not change.

Similar conductance oscillations were observed as function of a voltage V_{TG} applied to an added small top gate (TG) in the center of the FPI cell, with area ~0.75 μm^2 and circumference ~3 μm (see Fig. 4*A*). Again, the periodicities in V_{TG} for (1, 0) and (1/3, 0), are identical, as summarized in Fig. 4*B*. For

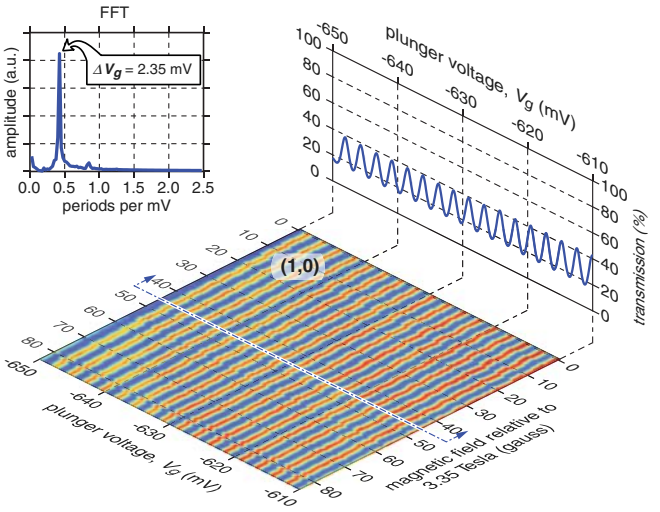

Fig. 2. Interference of the outer edge channel at $\nu = 1$ and $f_T = 0$. While independent of magnetic field, the transmission oscillates as function of plunger voltage, V_g. (*Upper Right*) A cut in the 2D B-V_g plot. (*Upper Left*) Fast Fourier transform of this cut with a periodicity of 2.35 mV, corresponding to the expulsion of one electron per period. Note that a weak second harmonic is also observable—corresponding to two fully rotating trajectories around the interferometer.

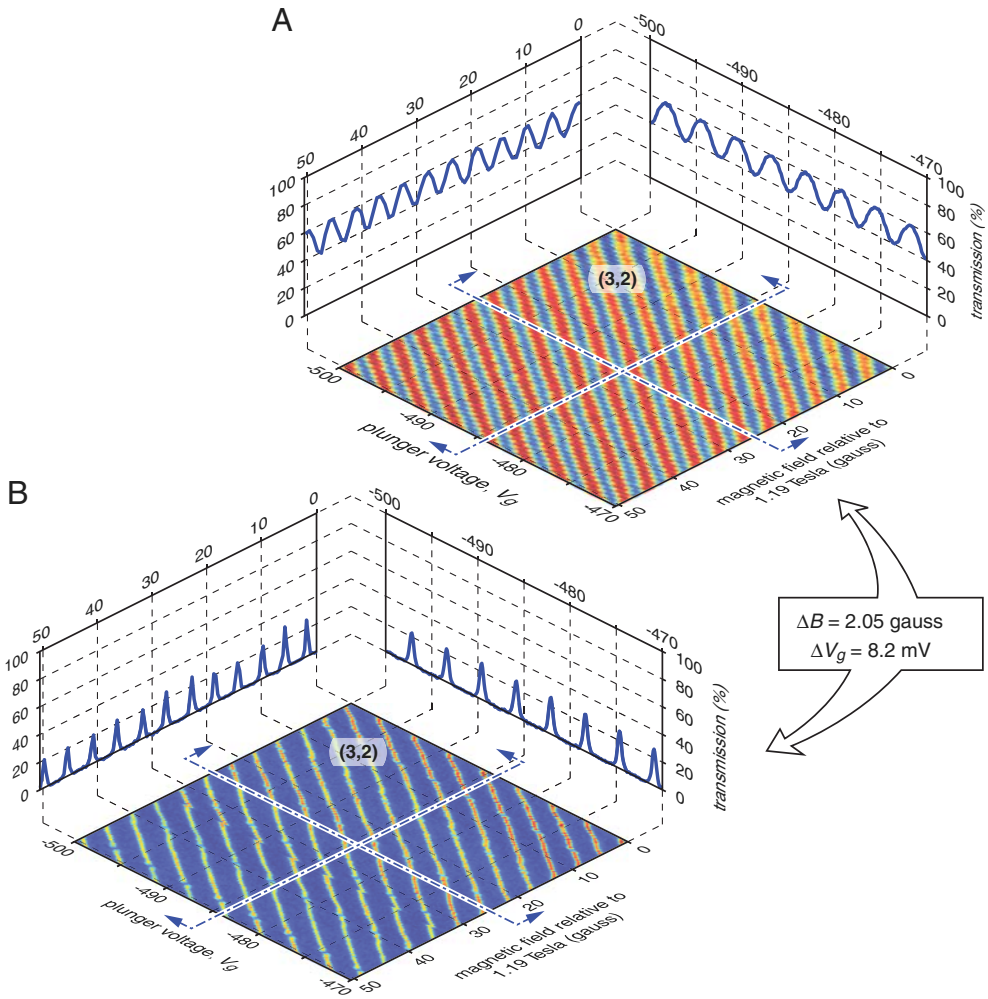

Fig. 3. Interference of an innermost channel at $\nu = 3$ and $f_T = 2$. (*A*) Color scale plot of interference in *B*-V_g plane with relatively open constrictions ($t \approx 0.7$), leading to a sine-like dependence of the transmission on *B* and V_g. The slope of the constant phase lines is opposite to the expected one if interactions between the electrons are negligible. (*B*) Color scale plot of interference in *B*-V_g plane with relatively pinched constrictions ($t \approx 0.3$), leading to sharp periodic peaks of the transmission. Note that the periodicities in both cases are identical.

$V_{TG} > -135$ mV, the area under the TG is being only partly depleted, and the periodicity observed is $\Delta V_{TG} \sim 0.23$ mV. A trivial two-plate capacitor model, with $C_{TG} \sim 0.66$ fF calculated for our specific device, suggests an expulsion of one electron in a single period. For $V_{TG} < -135$ mV, the 2DEG under the TG is fully depleted and the depletion region extends away from the TG. The capacitance of the TG to the 2DEG slowly decreases with negative gate voltage, starting at a periodicity of 0.23 mV and increasing to ~0.6 mV. The periodicity measured with a plunger gate for the $f_T = 0$ cases is about 2.3 mV. The ratio between the gate voltage periodicities of the plunger and the small TG corresponds exactly to the ratio between the plunger length (0.4 μm) and the TG perimeter (3 μm). This is consistent with ΔV_{TG} measured at beyond depletion voltages. A rather interesting behavior is observed in the V_g-V_{TG} plane when looking at the slope of the constant phase lines in Fig. 4*C*; both gates, plunger and top, lowered the area when biased negatively. We address this issue later.

We now discuss the FQHE regime, where interference was measured for $\nu = 4/3$, 2/3, 2/5, and 1/3. Due to space limitations, we discuss here only the latter two cases. Like in the IQHE, no interference oscillations were observed as function of *B* for cases with $f_T = 0$, namely, at (2/5, 0) and (1/3, 0). However, periodic oscillations of the conductance, as function of both *B* and V_g, were observed at (2/5, 1), as shown in Fig. 5. Although the quality of the data deteriorated somewhat, a fast Fourier transform of the bare data shows a single, reproducible, distinct peak, corresponding to $\Delta B = 9.2$ G and $\Delta V_g = 1.13$ mV (see Fig. 5*B*). We return to the analysis of this periodicity in *Discussion*.

Discussion

Model. The results discussed so far can be encapsulated as follows:

1. In each filling factor, any of the edge channels can be made to interfere independently of the others.
2. The periodicities ΔB and ΔV_g do not directly depend on the magnetic field (or the filling factor), nor the transmission coefficients t_1 and t_2, but only on f_T. The periodicity in magnetic field is solely determined by A and f_T:

$$\Delta B(B, V_g, f_T, t_1, t_2) = \Delta B(f_T) = -\frac{\phi_0}{A \cdot f_T}, \qquad [1]$$

as predicted in ref. 7 for the case $t_1, t_2 \ll 1$; here, however, we found it to hold for all values of the transmissions. Similarly, the periodicity in plunger gate voltage depends only on f_T:

$$\Delta V_g(B, V_g, f_T, t_1, t_2) = \Delta V_g(f_T), \qquad [2]$$

with ΔV_g monotonically increasing with increasing f_T (aside from two exceptions to be discussed below). Fig. 6 summarizes the measured periodicities ΔB and ΔV_g for IQHE and two cases of FQHE.

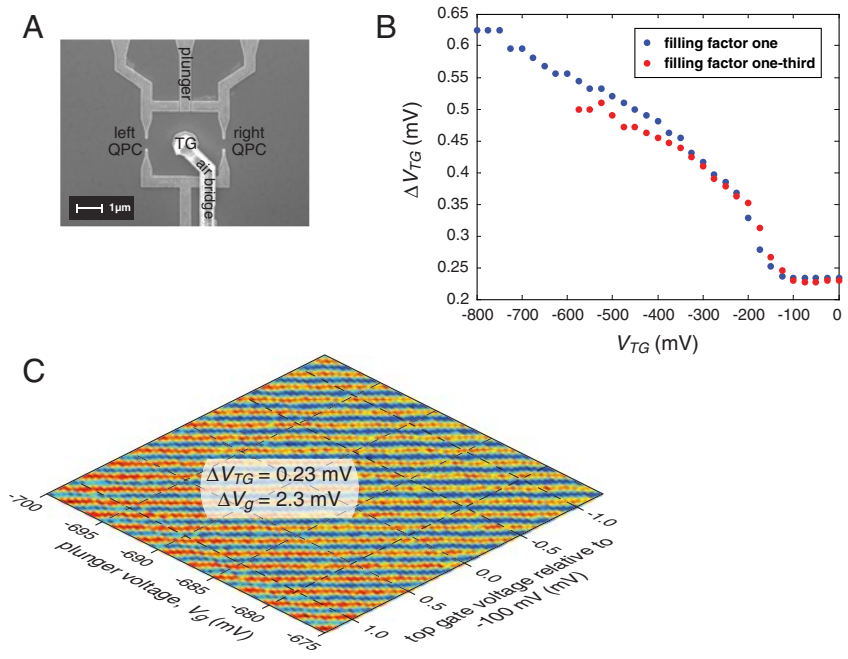

Fig. 4. Interference controlled by a voltage applied to a small top gate (deposited in the center of the FPI cell) and the plunger gate voltage. (*A*) SEM picture of the FPI with a small top gate. The brighter areas are metallic gates. (*B*) Periodicities of interference for $\nu = 1$ and $\nu = 1/3$ as function of gate voltage, before and after depletion under the gate. (*C*) Conductance in the plane of V_{TG}-V_g. Note that the two gates function in a similar fashion, namely, depleting the area under (and around) them leads to a decrease in the area of the interferometer.

3. For $f_T = 0$, the enclosed flux is independent of the magnetic field, indicating that the relevant area of the interferometer is proportional to $1/B$.

4. For $f_T > 0$, the enclosed flux decreases with increased magnetic field, indicating that the interferometer area shrinks faster than $1/B$ (hence, the minus sign in Eq. **1**).

The first, and most important, exception to these general statements is the periodicity ΔV_g in the case (2/5, 1): It is one-third of the measured value for all other configurations with $f_T = 1$. [Note that for $\nu = 2/5$, the case (2/5, 1) implies a fully transmitted outer channel of conductance $1/3(e^2/h)$.] The measurements were repeated for two separate devices and the results in both cases were identical. The second exception takes place for high filling factors, when a large number of channels are being trapped, such as (4, 0), (4, 1), and (5, 0). As seen in the example (4, 1) in Fig. 7, a "lattice-like" structure in the B-V_g plane appears instead of the more ubiquitous "pajama-like" stripes. The dependence on B and V_g is still periodic, but it cannot be described by a periodic function of a linear combination of B and V_g. This behavior is not yet understood.

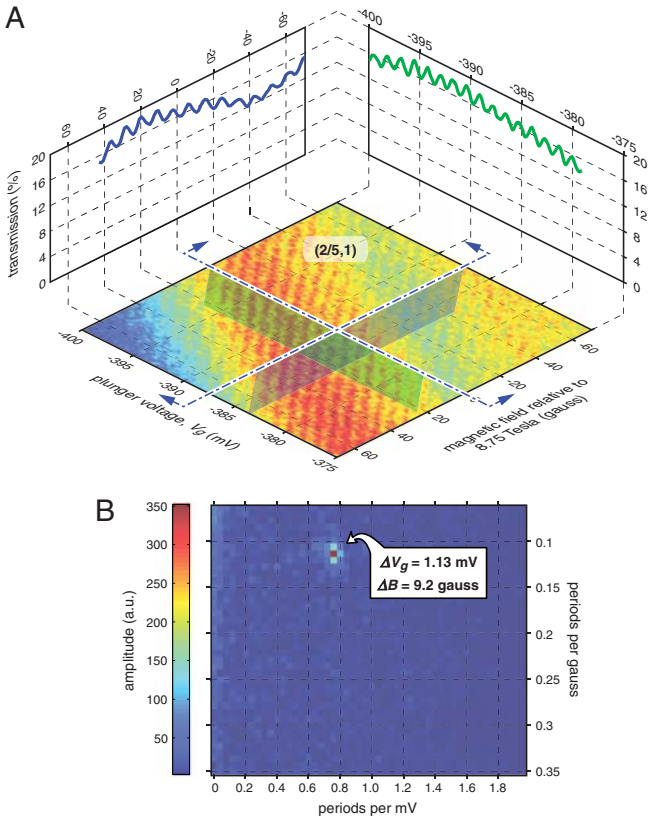

Fig. 5. Interference of the inner channel for bulk filling factor $\nu = 2/5$; case (2/5, 1). (*A*) Conductance plot in the B-V_g plane for the inner channel. (*Upper Left* and *Upper Right*) Traces with respect to B and V_g averaged over several traces. (*B*) 2D fast Fourier transform analysis of the interference oscillations. The periodicity in V_g, being one-third of that needed for expulsion of an electron, suggests the expulsion of $e/3$ charge per period, whereas the interfering quasiparticle is $e/5$ (see text).

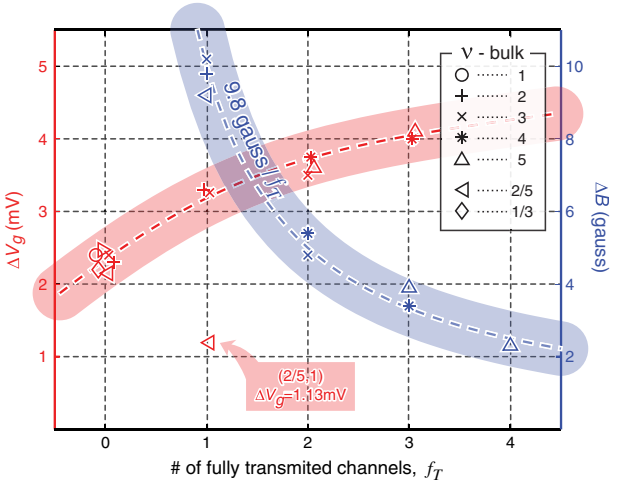

Fig. 6. Summary of the periodicities. In blue (*Left Axis*), periodicities in V_g as a function f_T, for different filling factors. A larger number of freely propagating outer channels screens the gate more efficiently, thus increasing the periodicities. In gray (*Right Axis*), periodicities in B as a function of f_T. The periodicities are inversely proportional to f_T.

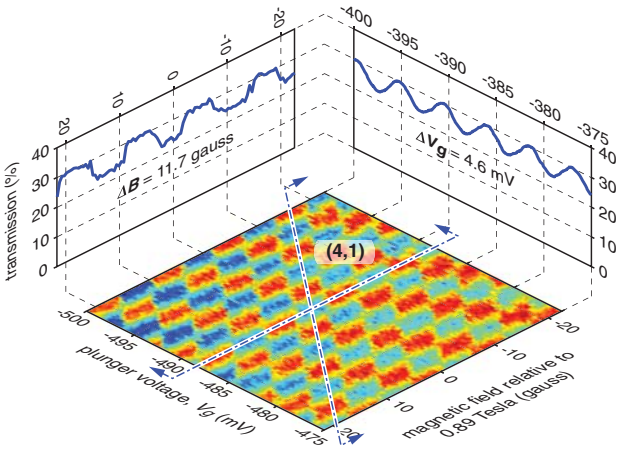

Fig. 7. Exotic behavior of the oscillations for case (4, 1), as an example of a typical behavior of many trapped channels in the FPI cell area. Here, there is a sinusoidal dependence on V_g (*Upper Right*), however, modulated by a square-type pulse train. Scanning B while keeping V_g fixed produces a sharp pulse train (*Upper Left*). Other cases, like (5, 0) and (6, 0), produce more complicated patterns.

Magnetic Field Periodicity. The empirical Eqs. **1** and **2** may be understood by means of a single physical assumption: The relevant area of the interferometer varies as the magnetic field is varied, namely, the magnetic flux through FPI area is $\Phi = B \cdot A(B, V_g)$, with A depending on V_g and B. Then, the flux evolves as function of B and V_g:

$$d\Phi = \frac{\partial(A \cdot B)}{\partial B} dB + \frac{\partial(A \cdot B)}{\partial V_g} dV_g = \left(A + B\frac{\partial A}{\partial B}\right) dB + B\frac{\partial A}{\partial V_g} dV_g, \quad [3]$$

with the lines of constant phase (constant flux) in the B-V_g plane given by

$$\frac{dB}{dV_g} = -\frac{B}{A}\frac{\partial A}{\partial V_g} \Big/ \left(1 + \frac{B}{A}\frac{\partial A}{\partial B}\right). \quad [4]$$

In earlier experiments with an electronic two-path MZI, we found that $\partial A/\partial B \approx 0$, with the lines of constant phase having an opposite slope from the one measured with the FPI (3, 15). Assume that all f_T fully transmitted channels enclose a similar area A_T. This area is expected to be field independent because the channels are in equilibrium with the leads. The inner channels are trapped and thus maintain a discrete and constant number of electrons N_R for small changes in B, while a smooth electron exchange can take place between the interfering channel and the fully transmitted ones. The total amount of charge in the interferometer cell is $Q = e[N_R + \frac{B}{\phi_0}(f_T A_T + A)]$. If charge neutrality is a major consideration, then Q should be independent of B, namely, $\partial Q/\partial B = 0$. Assuming $A \sim A_T$,

$$\frac{\partial(AB)}{\partial B} = -f_T \cdot A, \quad [5]$$

implying that the flux, and hence the AB phase, indeed *decreased* with increasing magnetic field at a rate proportional to f_T and were independent of B for $f_T = 0$—as observed in both the integer and fractional cases.

For $f_T = 0$, increasing B is followed by a decrease in the area A in such a way that the flux, and hence the number of occupied states, are kept constant, but the charge density at the center of the FPI cell grows. A spatial imbalance between electrons and ionized donors takes place. Increasing the field further must lead eventually to relaxation of that imbalance by creation of a hole within the interfering Landau level if this is also the only edge channel, or electron tunneling from the trapped channels otherwise. In any case, this leads to abrupt increase of one quantum flux to the interfering loop (hence, invisible in the interference pattern). The area "breathes" with the magnetic field. It decreases monotonically and increases abruptly while keeping the average constant. The same holds for $f_T > 0$. The only difference is that the area decreases with increasing B even faster, because the interfering channel loses charge monotonically to the f_T lower filled Landau levels (whose density of states increases with field) leading to the positive slope of the constant phase lines in the B-V_g plane.

Gate Voltage Periodicity. The periodicity in gate voltage ΔV_g, and in particular its relation to the fractional filling factor ν, provide an insight to the charge of the interfering quasiparticle. The dependence on V_g can be understood if we assume that the capacitance C between the plunger gate and the interfering channel depends only on the number of fully transmitted channels (that screen the plunger gate voltage), namely, $C = C(f_T)$. The interfering channel flows at the interface between two areas with different filling factors, ν_{out} and ν_{in}, each with charge q_i per flux quantum $q_i = e\nu_i$. (For example, for the case (3, 1) we have $\nu_{\text{out}} = 1$ and $\nu_{\text{in}} = 2$, while (1/3, 0) relates to $\nu_{\text{out}} = 0$ and $\nu_{\text{in}} = 1/3$.) As long as the sole function of biasing the plunger gate by δV_g is to move the interface between the two filling factors by area δA, and thus expel charge δq from within the interferometer, we may write

$$\delta q = C\delta V_g = \frac{B \cdot \delta A}{\phi_0} \cdot e(\nu_{\text{in}} - \nu_{\text{out}}). \quad [6]$$

Assuming that the change in area does not change the number of quasiparticles enclosed by the interfering loop (as their number is very small near the center of the conductance plateau), the change of area leads to a change in the AB phase,

$$\delta\phi = 2\pi\frac{e^*}{e}\frac{B \cdot \delta A}{\phi_0}. \quad [7]$$

Using Eq. **6**, we get a relation between the interfering quasiparticle charge e^* and the periodicity ΔV_g:

$$\frac{e^*}{e} = \frac{\nu_{\text{in}} - \nu_{\text{out}}}{\Delta V_g / V_e}, \quad [8]$$

with $V_e \equiv e/C$ the gate voltage needed to expel one electron.

Look first at cases (1/3, 0) and (2/5, 0), both with a gate voltage periodicity $\Delta V_g \sim 2.2$ mV (which is the similar value as for $f_T = 0$ in the integer cases). Evidently, with the assumption $C = C(f_T)$, with C being independent of the filling factor, the measured expelled charge per period must be in both cases e. Because the interfering edge channel in both cases belongs to the one-third fractional state, $\nu_{\text{in}} - \nu_{\text{out}} = 1/3$, and the interfering quasiparticle charge, deduced directly from Eq. **8**, must be $e^* = e/3$, agreeing with our expectations.

What happens in the case (2/5, 1), where the interfering channel belongs to the two-fifths fractional state? The observed periodicity is $\Delta V_g \sim 1.13$ mV (see Fig. 5)—nearly one-third of the period observed in the integer cases (ν, 1). Because the capacitance $C(f_T = 1)$ was found to be independent of filling factor, and the measured periodicity is one-third of that observed in the integer regime, the expelled charge per period of the oscillation must be $e/3$ (directly proportional to ΔV_g). Again, for $\nu_{\text{in}} - \nu_{\text{out}} = 2/5 - 1/3 = 1/15$ in this case, and the above periodicity, the interfering charge is $e^* = e/5$. This is a striking example of

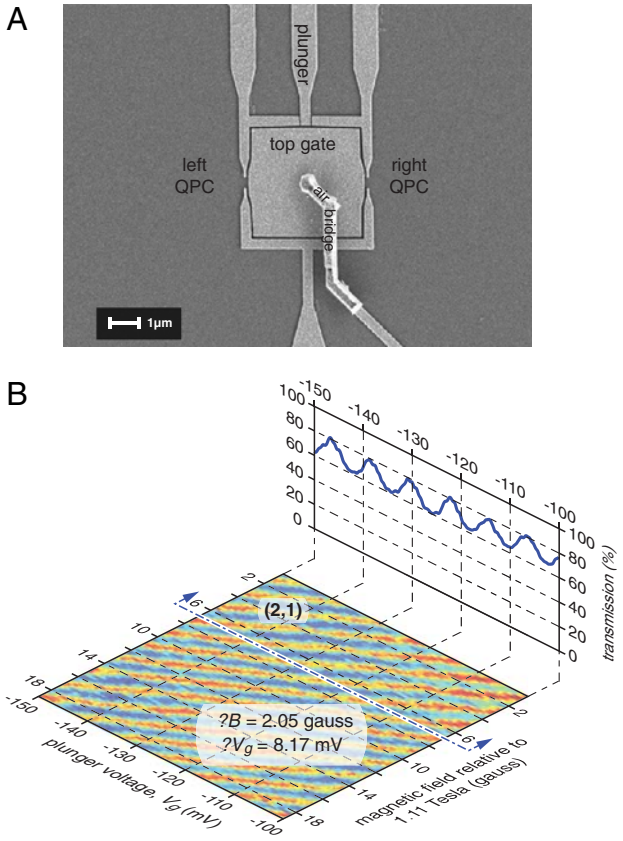

Fig. 8. Behavior of an FPI covered by a grounded top gate covering the full area of the interferometer. (*A*) SEM image of the larger FPI (active area ~17 μm^2) with the top gate. (*B*) Conductance in the B-V_g plane for case (2, 1) exhibiting an opposite slope of the constant phase lines in the uncovered interferometer.

an expelled charge $e/3$ per period of gate voltage, while the interfering quasiparticles carried charge $e/5$.

Because the periodicity of the oscillations is independent of t_1 and t_2, one can invoke a simpler explanation (7) for the expelled charge in each period, which is valid only in the Coulomb blockaded limit, namely, when t_1 and $t_2 \ll 1$. In that limit, the charge enclosed by the constrictions must be quantized in units of the elementary charge in the incompressible regions within the two constrictions. For cases (1/3, 0) and (2/5, 0), the filling factor within the constrictions is zero and the expelled charge is that of the electron, as indeed was observed. Alternatively, for (2/5, 1), the filling factor in the constrictions is one-third and the expelled charge must be $e/3$; again, agreeing with the observation.

Top Gated Device. The significance of Coulomb interactions in the FPI was tested by adding a grounded metal gate that fully covered the FPI's area [large top gate (LTG)], as was also done in ref. 18. This gate effectively increased the screening of the uncompensated charges. Although the addition of the LTG to the smaller FPI (area 4.4 μm^2) did not affect the orientation of the constant phase lines (it did increase the periodicity in plunger gate voltage, which is expected because the plunger gate is less effective due to screening provided by the LTG biasing), adding an LTG to the larger FPI (area 17.6 μm^2, as seen in Fig. 8*A*) led to markedly different results. First, unlike *all* of our previous results, AB oscillations were measured as function of magnetic field also for cases with $f_T = 0$, such as (2, 0) and (1, 0). Second, as seen in Fig. 8*B* for the case (2, 1), the orientation of the constant phase lines in the B-V_g plane was reversed, indicating an increased flux with increasing magnetic field (see also ref. 18). However, the area determined from the AB periodicities in B still did not match the expected area.

Conclusion

Our experiments provide a detailed first step study toward the realization of interferometers that might give direct evidence of the statistics of fractionally charged quasiparticles. Our studies covered interference of the different edge channels of complex edge structures in integer and a few fractional states in the QHE regime. We found that the interferometers are very strongly affected by Coulomb interactions, which radically modify the interferometer area with magnetic field—independent of the coupling strength to the leads (in or away from the Coulomb blockade regime). Interfering charges of 1e, $e/3$, and $e/5$ where deduced from the interference patterns.

ACKNOWLEDGMENTS. We are grateful to B. I. Halperin, C. Marcus, I. Neder, B. Rosenow, A. Yacoby, and Y. M. Zhang for helpful discussions. We acknowledge the partial support of the Israeli Science Foundation, the Minerva foundation, the German Israeli Foundation, the German Israeli Project Cooperation, the European Research Council under the European Community's Seventh Framework Program (FP7/2007-2013)/ERC grant agreement 227716, the US-Israel Bi-National Science Foundation, and Microsoft's Station Q; N.O. acknowledges support from the Israeli Ministry of Science and Technology.

1. Nayak C, et al. (2008) Non-abelian anyons and topological quantum computation. *Rev Mod Phys* 80:1083–1159.
2. Schuster R, et al. (1997) Phase measurement in a quantum dot via a double-slit interference experiment. *Nature* 385:417–420.
3. Neder I, et al. (2007) Interference between two indistinguishable electrons from independent sources. *Nature* 448:333–337.
4. Willet RL, Pfeiffer LN, West KW (2009) Measurement of filling factor 5/2 quasiparticle interference: Observation of charge e/4 and e/2 period oscillations. *Proc Natl Acad Sci USA* 106:8853–8858.
5. Camino FE, Zhou W, Goldman VJ (2007) Quantum transport in electron Fabry-Perot interferometer. *Phys Rev B* 76:155305 1–6.
6. Godfrey DM, et al. (2007) Aharonov-Bohm-like oscillations in quantum Hall corrals. arXiv:0708.2448.
7. Rosenow B, Halperin BI (2007) Influence of interactions on flux and back-gate period of quantum Hall interferometers. *Phys Rev Lett* 98:106801.
8. Martin J, et al. (2004) Localization of fractionally charged quasi-particles. *Science* 305:980–983.
9. Kitaev A (2003) Fault-tolerant quantum computation by anyons. *Ann Phys* 303:2–30.
10. Nayak C, Simon SH, Stern A, Freedman M, Das Sarma S (2007) Non-abelian anyons and topological quantum computation. arXiv:0707.1889.
11. Das Sarma S, Freedman M, Nayak C (2005) *Phys Rev Lett* 94:166802 1–4.
12. Bonderson P, Kitaev A, Shtengel K (2006) Detecting non-abelian statistics in the $\nu = 5/2$ fractional quantum Hall state. *Phys Rev Lett* 96:016803 1–4.
13. Stern A (2008) Anyons and the quantum Hall effect-A pedagogical review. *Ann Phys* 1:204–249.
14. Chamon C, et al. (1997) Two point-contact interferometer for quantum Hall systems. *Phys Rev B* 55:2331–2343.
15. Ji Y, et al. (2003) An electronic Mach-Zehnder interferometer. *Nature* 422:415–418.
16. Law KT, Feldman DE, Gefen Y (2006) Electronic Mach-Zehnder interferometer as a tool probe fractional statistics. *Phys Rev B* 74:045319 1–16.
17. Van Wees BJ, et al. (1989) Observation of zero-dimensional states in a one-dimensional electron interferometer. *Phys Rev Lett* 62:2523 1–4.
18. Zhang Y, et al. (2009) Distinct signatures for coulomb blockade and Aharonov-Bohm interference in electronic Fabry-Perot interferometers. *Phys Rev B* 79:241304 1–4.